Homogeneous Fluorescence-Based DNA Detection with Water-Soluble Conjugated Polymers

Bin Liu* and Guillermo C. Bazan*

Departments of Chemistry and Materials, Institute for Polymers and Organic Solids, University of California, Santa Barbara, California 93106

Received March 12, 2004. Revised Manuscript Received July 1, 2004

Methods for real-time, high-sensitivity polynucleotide detection are of vast scientific and economic importance. Homogeneous biosensor assays that take advantage of the collective response of water-soluble conjugated polymers and the self-assembly characteristic of aqueous polyelectrolytes have shown potential for improvements over small molecule methods. Cationic polythiophenes transduce oligonucleotide hybridization into a colorimetric output based on conformational changes of the polymer upon interaction with single-stranded DNAs or double-stranded DNAs. Cationic poly(fluorene-*co*-phenylene) materials serve as donors in fluorescence energy-transfer assays which display signal amplification. Signal transduction in aqueous media is controlled by specific electrostatic interactions.

Introduction

Methods for real-time, high-sensitivity polynucleotide detection are of vast scientific and economic importance.[1−3] Novel techniques that determine DNA hybridization and sequence characterization are therefore under intense investigation[1−4] for applications, such as medical diagnostics, identification of genetic mutations, gene delivery monitoring, and specific genomic techniques.[5] DNA-related technologies will increase in importance as samples from patients need to be quickly screened and compared against genomic data.

Effective DNA-sensing requires selectivity, to identify single-nucleotide polymorphism (SNPs), and sensitivity, to provide information from the small quantities of naturally occurring DNAs. A variety of optical and electrochemical DNA hybridization sensors have therefore been proposed,[6] including DNA microarray technologies, which rely on the hybridization between DNA sequences on a microarray surface,[7] the use of semiconductor crystals or quantum dots as fluorescent probes,[8−10] detection based on nanoparticle-ampilified surface plasmon enhanced signals,[11−13] and the use of redox-active nucleic acids.[14] Homogeneous fluorescence-based assays,[15,16] although established for some time, remain of paramount importance, principally because of their high sensitivity and ease of operation.[17] Cationic organic dyes such as ethidium bromide and thiazole orange, which are strongly emissive only when intercalated within the grooves of double-stranded DNA (dsDNA), serve as direct DNA hybridization probes, but lack sequence specificity.[18,19] Traditional energy/electron-transfer pairs for strand-specific identification require chemical labeling of two nucleic acids, or dual modification of the same altered strand (for example, molecular beacons).[20,21] Difficulties in labeling two DNA sites give rise to low yields and singly labeled impurities, which lower detection sensitivity.

* To whom correspondence should be addressed. E-mail: bliu@chem.ucsb.edu; bazan@chem.ucsb.edu.

The chemical structures of conjugated polymers (CPs) offer several advantages as the responsive basis for chemical and biological detection schemes based on optical methods. These materials may be viewed as a collection of short, conjugated (oligomeric) units kept in close proximity by virtue of the polymer backbone. Their structure allows for effective electronic coupling and therefore fast intra- and interchain energy transfer.[22] CP-based sensors are sensitive to minor perturbations, due to amplification by the collective response, and therefore can offer advantages when compared with small molecule counterparts.[23,24b,24c] This collective response influences optoelectronic properties, such as Förster resonance energy transfer (FRET), electrical conductivity, and fluorescence efficiency, properties which can be used to report, or "transduce", target analyte presence.[24b,24c.] Electrochemical and optical DNA sensors based on CPs such as poly(pyrrole), poly(thiophene), poly(phenylenevinylene), etc. have been reported,[24] including oligonucleotide-functionalized CPs that transduce hybridization events into electrical signals without analyte labeling.[25] An assay using a cationic conjugated polymer, which does not require chemical labeling of the nucleic acid or covalent attachment of the DNA probe (reporter), has also been reported.[26]

Water solubility, a prerequisite for interrogating biological substrates, is typically achieved by attaching charged pendant groups onto the CP backbone.[27] Recent publications have reviewed the synthesis and properties of these conjugated polyelectrolytes, including those containing poly(thiophene), poly(*p*-phenylene), poly(phenylenevinylene), and poly(phenyleneethynylene) backbones.[27,28] The molecular structures of typical water-soluble CPs are shown in Figure 1. It is noteworthy that the charged nature of these structures permits coordination of electrostatic forces with oppositely charged analyte targets.[29,30]

The focus of this contribution is to review CP-based DNA sensors in homogeneous media. Two main classes

10.1021/cm049587x CCC: $27.50
Published on Web 09/11/2004

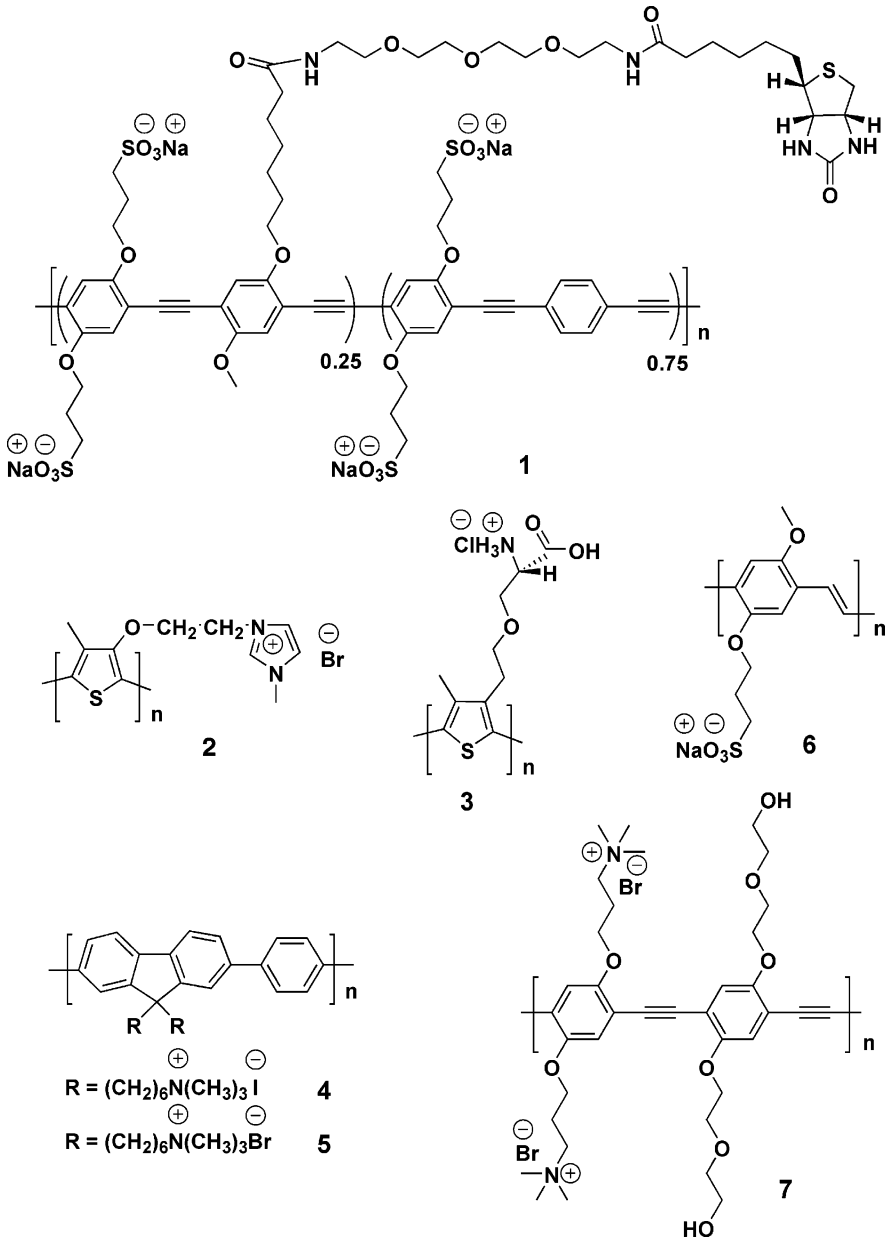

Figure 1. Examples of water-soluble CPs used in biosensor applications.

of polymers have been used, namely, cationic poly(thiophene)s and cationic poly(fluorene-*co*-phenylene)s. For organizational purposes, each class will be discussed separately.[31] We examine the biosensing mechanism, with special attention to the varying contributions of hydrophobic and electrostatic forces. Fine-tuning of CP structures to improve detection sensitivity and selectivity will also be addressed.

Cationic Poly(thiophene)s—DNA Detection Based on Main Chain Conformational Perturbations

This methodology provides the advantage that it does not require chemical functionalization of probes or analytes. It has two components: a cationic poly(thiophene) and a probe oligonucleotide. Detection is based on different electrostatic interactions and conformational structures between cationic poly(3-alkoxy-4-methylthiophene)s and single-stranded DNAs (ss-DNA) or hybridized ds-DNA. For example, polymer **2** in Figure 1 in buffer provides a yellow solution (λ_{max} = 397 nm), corresponding to a random-coil conformation.[24a] When a capture ss-DNA is added, the mixture appears red in color (λ_{max} = 527 nm) because of CP/ss-DNA complexation. Upon addition of a ss-DNA complementary to the capture strand, triplex formation results in a return to the yellow color (λ_{max} = 421 nm).

A slight but distinct change in the absorption spectrum is observed in the case of a ss-DNA target with two base mismatches, as compared to using perfectly complementary ss-DNA. Even with only one base mismatch, it is possible to distinguish between perfect and nonperfect hybridization. In this case, the colorimetric difference is mainly based on different complexation kinetics since similar yellow solutions are observed after 30−60 min of mixing at 55 °C. However, it is possible to stop the hybridization reaction after 5 min of mixing, by placing the solutions at room temperature. When

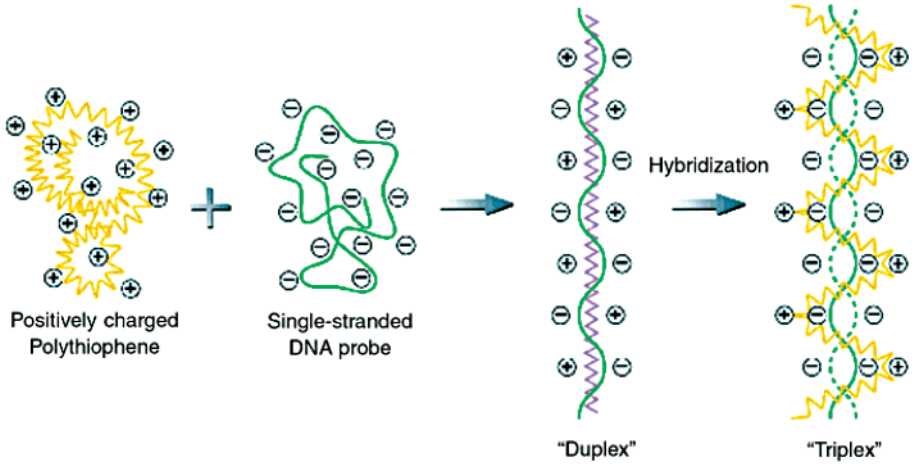

Figure 2. Schematic description of the formation of poly(thiophene)s/ss-DNA duplex and poly(thiophene)/ds-DNA triplex complexes. Figure used with permission.[26]

these procedures are followed, stable yellow and orange solutions are observed.[32]

It is believed that these colorimetric changes are made possible by the different conformational structures of the CP in the duplex form (highly conjugated, planar conformation) compared to that observed in the triplex form (less conjugated, nonplanar form). Single mismatch detection is possible by taking advantage of the difference in complexation rates and the effect of hybridization levels on polymer absorption characteristics. A schematic description of duplex and triplex formation is shown in Figure 2. Circular dichroism measurements show no optical activity for the CP in its random coil and in the duplex form, but show a bisignate spectrum centered at 420 nm in the triplex form, corresponding to a right-handed helical polymer backbone orientation.[24d]

These conformational changes can also be detected by fluorescence spectroscopy. Polymer **2** has a fluorescence quantum yield of approximately 0.03 in a 0.1 M NaCl aqueous solution. Upon addition of 1.0 equiv (on a per charge basis) of the capture ss-DNA probe, the fluorescence intensity decreases and the emission red-shifts. Formation of a polymeric triplex leads to a 5-fold increase of intensity. Overall, these experiments show that cationic poly(thiophene) derivatives can easily transduce oligonucleotide hybridization into an optical output that can be used for DNA identification.[33] Use of poly(thiophene) transduction has shown zeptomole sensitivity using a custom-made detection instrument.[34]

A study of the poly(3-[(*S*)-5-amino-5-carboxyl-3-oxapentyl]-2,5-thiophene hydrochloride) (polymer **3** in Figure 1) shows that hydrogen bonding can couple with electrostatic forces in determining the organization the final DNA/CP complex. Electrostatic attraction between the CP and the ss-DNA disrupts the internal H-bonding within the polymer, planarizes the structural relationship between monomeric units, and leads to the appearance of a new emission band at 595 nm. The DNA bases subsequently form hydrogen bonds with the amino and carbonyl groups of nearby CP chains, resulting in aggregation of polymer chains, and the appearance of a further red-shifted emission band at 670 nm. Addition of a complementary DNA strand to the ss-DNA/polymer **3** complex causes the emission to shift to 585 nm, with an increase in intensity. Since the complementary bases form hydrogen bonds with each other, the hydrogen bonding between the polymer chain and the ss-DNA is disrupted.

Cationic Poly(fluorene-*co*-phenylene)s—DNA Detection Based on Fluorescence Resonance Energy Transfer (FRET)

A method for DNA analysis based on optically amplified FRET from a donor CP to a signaling chromophore recently appeared.[35] The assay contains two ingredients: (a) a light harvesting CP and (b) a probe oligonucleotide attached to a luminescent signaling chromophore (C*). Emission of light characteristic of the signaling C*, upon excitation of the CP, indicates the presence of the target oligonucleotide. Transduction by electrostatic interactions, followed by energy transfer, is an essential component of the general strategy.

As shown by Förster,[36] dipole—dipole interactions lead to long-range FRET from a donor to an acceptor chromophore. Equation 1 describes how the rate of energy transfer depends on the donor—acceptor distance (r), the orientation factor (κ), and the overlap integral (J).

$$k_{t(r)} \propto \frac{1}{r^6} \cdot \kappa^2 \cdot J(\lambda) \qquad (1)$$

$$J(\lambda) = \int_0^\infty F_D(\lambda)\epsilon_A(\lambda)\lambda^4 \, d\lambda$$

The light-harvesting CP and the signaling C* correspond to the donor and acceptor, respectively. The absorption bands of CP and C* are chosen to have minimal overlap and the luminescent emission spectra of the two species occur at clearly differentiated wavelengths.

A scheme for detecting PNA/DNA interactions based on the FRET conditions given above is shown in Scheme 1.[35] Consider a solution that contains a cationic CP (CCP, shown in black) and a PNA strand (shown in red) labeled with fluorescein (C*). Since PNA is neutral, there are no electrostatic interactions, resulting in an average CCP- - -PNA-C* distance too large for effective FRET. Upon addition of ss-DNA, one can encounter two situations. Situation **A** corresponds to addition of a complementary ss-DNA (shown in blue), which hybridizes with the target PNA. Hybridization of the neutral PNA-C* probe and the negatively charged ss-DNA

Scheme 1. Schematic of the CCP/PNA-C*/DNA Sensor Operation

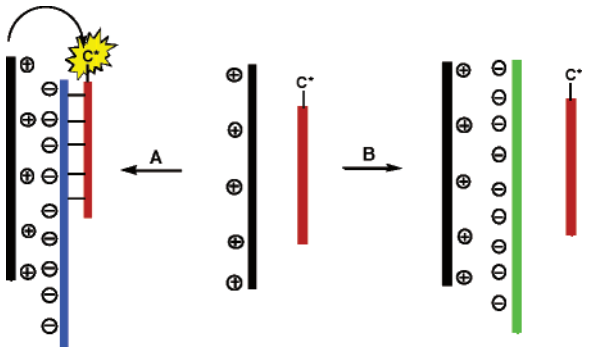

Scheme 2. Modified Schematic DNA-C*/DNA Sensor Operation

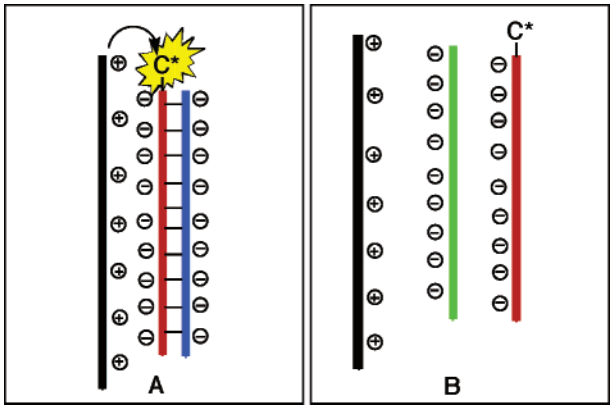

target produces a macromolecule with a net negative charge and results in favorable electrostatic interactions between the hybrid complex and the CCP. Distance requirements for FRET are thus met only when ss-DNA of complementary sequence to the PNA-C* probe is present. When a ss-DNA that does not match the PNA sequence is added (shown in green), situation **B**, hybridization does not take place; electrostatic complexation occurs only between the CCP and the ss-DNA while the CCP- - -PNA-C* distance remains too large for FRET. PNA/ss-DNA hybridization can therefore be measured by the FRET efficiency or by the enhanced C* emission. The overall scheme serves as a probe for the presence of ss-DNA that matches the PNA sequence.

Scheme 1 was tested using the water-soluble CCP poly(9,9-bis(6′-*N,N,N*-trimethylammonium)-hexyl)-fluorene phenylene) containing iodide counterions (**4** in Figure 1).[37] A PNA probe (5′-CAGTCCAGTGATACG-3′) with fluorescein at the 5′ position was used as PNA-C* (red fragment in Scheme 1). Intense fluorescein emission was observed at the presence of a complementary strand, while only a minor signal was observed for a noncomplementary strand upon excitation of the CCP at 380 nm. Signal amplification by the CCP provides a fluorescein emission that is over 25 times higher than that obtained by the direct excitation of the dye at its absorption maximum. This amplification reflects the higher optical density of the polymer, and the very efficient FRET step.

Scheme 1 was subsequently modified to use C*-labeled ss-DNA as the signaling reporter.[38] While the use of PNA is well-established, the purification of ss-DNA is more straightforward. Scheme 2 shows the

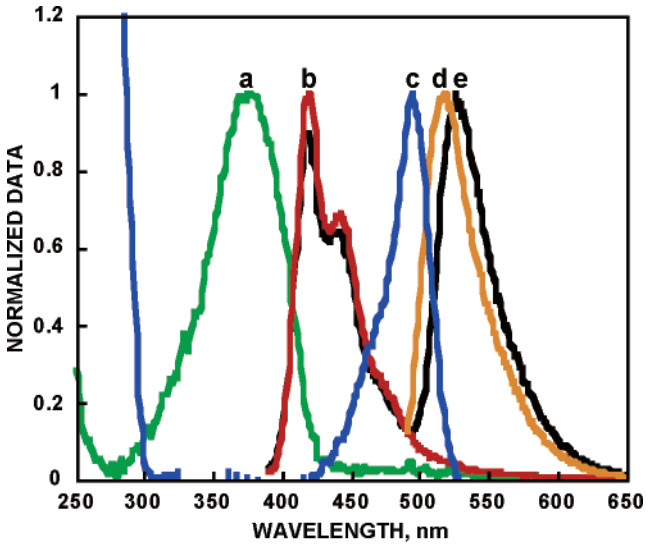

Figure 3. Absorption [(a) green and (c) blue] and emission [(b) red and (d) orange] spectra of polymer **4** [(a) and (b)] and ss-DNA$_1$-C* [(c) and (d)] upon excitation at 380 and 480 nm, respectively. The emission of the energy-transfer complex [(e) black] excited at 380 nm is also shown ([**4**] = 8.41×10^{-7} M, [ss-DNA$_1$-C*] = 2.1×10^{-8} M).

two situations encountered when using ss-DNA-C* (shown in red) and a complementary strand (in blue, situation A) or a noncomplementary strand (in green, situation B), when in the presence of a CCP (in black). In the case of a noncomplementary strand, nonhybridized strands will interfere with the ss-DNA-C*- - -CCP interactions. Based exclusively on these considerations, closer proximity between the optical units should take place with the "target" strand in situation A.

The absorption and emission spectra of **4** and ss-DNA$_1$-C* (5′-C*-GTA AAT GGT GTT AGG GTT GC-3′, where C* = fluorescein) (Figure 3) show an optical window for selective excitation of **4**, between the absorption of DNA and C*. The emission of **4** overlaps the absorption of C*, and in a solution of **4** and ss-DNA$_1$−C*, excitation of **4** at 380 nm therefore results in efficient FRET to C*.

A comparison of the fluorescence from solutions with **4** and ss-DNA$_1$-C* previously treated with complementary ss-DNA$_2$ (5′-CAT CTG TAA ATC CAA GAG TAG CAA CCC TAA CAC CAT TTA C-3′) and noncomplementary ss-DNA$_3$ (5′-AAA ATA TTG TGT ATC AAA ATG TAA ATG GTG TTA GGG TTG C-3′) revealed a higher FRET ratio for the hybridized DNA (Figure 4). These data show that situation **A** in Scheme 2 indeed leads to higher FRET ratios and that CCPs can be used to monitor the presence of a complementary strand to ss-DNA$_1$-C*. The main difference for Scheme 2, relative to Scheme 1, is that there is residual ss-DNA-C*/CCP binding when the noncomplementary strand is present, which leads to sensitized dye emission. The result is a stronger background signal, compared with using PNA-C*, which does not bind to the CCP to any appreciable extent.

It is also highly significant that these optical differences are observed in the presence of a buffer containing 10 mM sodium citrate and 100 mM NaCl. Buffer ions screen negative charges on DNA, which facilitates hybridization, but weaken electrostatic interactions between CPs and oppositely charged fluorescence ac-

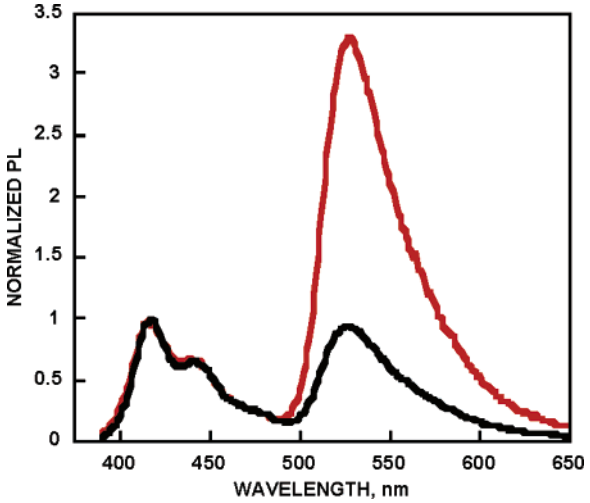

Figure 4. Emission spectra of **4** with hybridized (ss-DNA$_1$-C*/ss-DNA$_2$, red) and nonhybridized (ss-DNA$_1$-C* + ss-DNA$_3$, black) DNA probes in SSC buffer. The spectra were normalized to polymer emission.

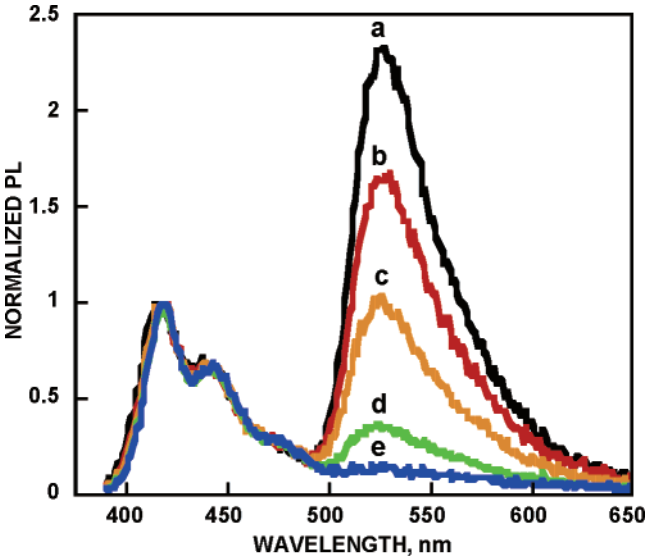

Figure 5. Effect of [NaCl] on the FRET between hybridized ss-DNA$_1$-C*/ss-DNA$_2$ and **4**. [NaCl] ranges from the initial buffer concentration (0.100 M NaCl) to 1.238 M, with a = 0.110 M, b = 0.316 M, c = 0.397 M, d = 0.597 M, and e = 1.238 M.

ceptors.[39] Multiple charge interactions between **4** and the DNA molecules are capable of compensating for this screening effect.

The Coulobic potential between charged surfaces of low potential is often approximated using the Debye–Hückel equation,

$$\psi_x \approx \psi_o e^{-\kappa x}$$

where ψ_o is the surface potential and $1/\kappa$ represents the characteristic Debye length. The Debye length in aqueous solutions can be determined by the Grahame equation which, simplified for 1:1 electrolyte solutions such as NaCl, is given as[39]

$$\frac{1}{\kappa} = \frac{0.304}{\sqrt{[\mathrm{NaCl}]}}\ \mathrm{nm}$$

Increasing the concentration of NaCl thus decreases, or collapses, the electrostatic layer of counterions, resulting

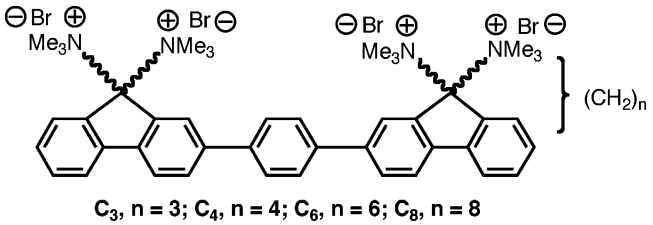

Figure 6. Structures of water-soluble oligomers with varying distances between the optically active fragment and the cationic groups.

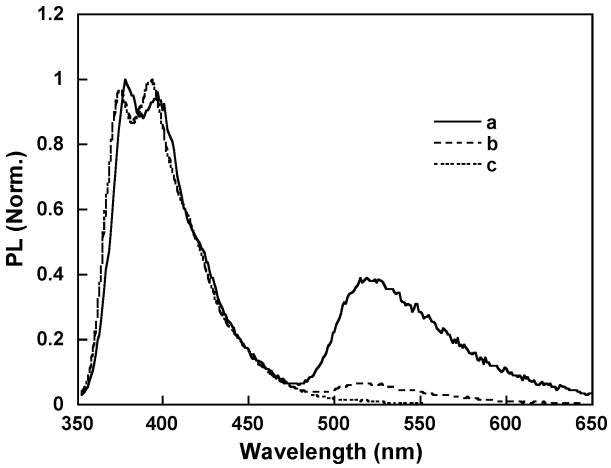

Figure 7. Effect of ionic strength on the FRET between **C$_3$** and ss-DNA$_4$-C*. The emission of **C$_3$** is normalized for comparison. The concentration of NaCl ranges from 0 to 0.1 M, with a = 0 M, b = 0.02 M, and c = 0.1 M.

in an exponential decrease in the potential between the two surfaces. This is often referred to as electrostatic screening.

According to Debye–Hückel Theory, if the NaCl concentration increases, the attraction between oppositely charged polymers decreases and should result in a decrease in energy transfer. In buffer (0.11 M salt) the electrostatic potential is sufficiently strong to bring hybridized DNA ([ss-DNA$_1$-C*/ss-DNA$_2$] = 2.1×10^{-8} M) and **4** (2.1×10^{-7} M), as seen in Figure 4. Subsequent increases in the concentration of NaCl result in a FRET decrease, as shown in Figure 5, which highlights the importance of electrostatic forces in determining **4**/DNA proximity.[40]

To further elucidate the driving force for CCP/DNA-C* binding, a series of fluorene-phenylene oligomers with varying distances between the charged groups and the optically active conjugated fragment was synthesized.[41] The general structure of these molecules is shown in Figure 6.

In buffer, only the **C$_6$**/ss-DNA$_4$-C* and **C$_8$**/ss-DNA$_4$-C* (5′-C*-CCA ATC AGT CCA GTG ATA CG-3′, C* = fluorescein) combinations show FRET to C*. However, energy transfer from **C$_{3-8}$** to ss-DNA$_4$-C* is observed in water. The absence of buffer ions allows electrostatic forces to bring the two oppositely charged molecules into close proximity.[42] Addition of NaCl to **C$_3$**/ss-DNA$_4$-C* solutions results in a decrease of C* emission and an increase of **C$_3$** emission (Figure 7). Note that the data in Figure 7 are normalized relative to oligomer emission to highlight the relative decrease in C* emission. At 0.1 M NaCl, C* emission is absent, indicating ionic screening of the **C$_3$**/ss-DNA-C* attraction. For the

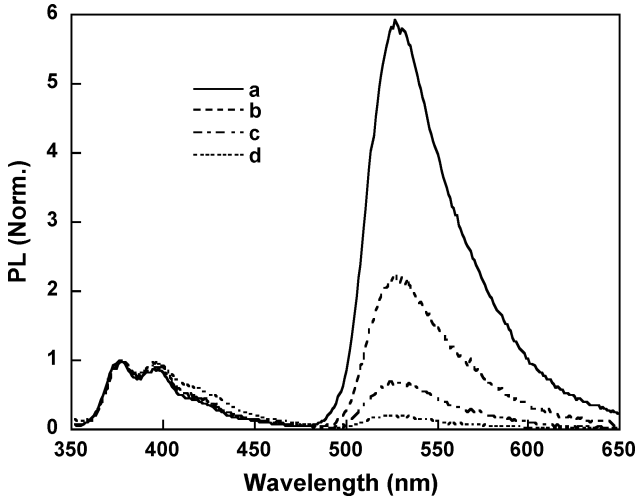

Figure 8. Effect of ionic strength on the FRET between $\mathbf{C_8}$ and ss-DNA_4-C*. The emission of $\mathbf{C_8}$ is normalized for comparison. The concentration of NaCl ranges from 0 to 1.07 M, with a = 0 M, b = 0.20 M, c = 0.46 M, and d = 1.07 M.

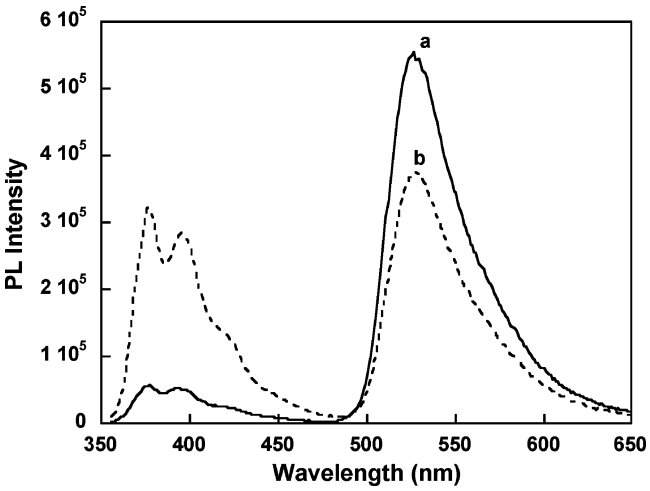

Figure 9. Fluorescence from solutions containing $\mathbf{C_8}$ and (a) ss-DNA_5-C* and (b) hybridized DNA_5-C* probes in buffer ([ss-DNA_5-C*] or [hybridized DNA_5-C*] = 2.0×10^{-8} M, [$\mathbf{C_8}$] = 1.2×10^{-7} M). The excitation wavelength was 345 nm.

$\mathbf{C_8}$/ss-DNA_4-C* mixture, when the NaCl concentration reaches 0.2 M, only 30% of the emission from fluorescein is lost, and it is still detectable when [NaCl] = 1.0 M (Figure 8). The effect of salt addition on electrostatic screening in Figures 7 and 8 shows that hydrophobic interactions are important and more prevalent for $\mathbf{C_8}$. This dependence on structure is in agreement with Bloomfield's calculations to determine the roles of electrostatics and hydrophobicity in the binding of cationic lipids to DNA.[43]

When compared to ss-DNA, ds-DNA has a more rigid and more compact structure and exhibits an increased charge density.[44] In ds-DNA, the hydrophobic bases are packed inside the helix, which minimizes external hydrophobic interactions.[45] To understand the effect of these structural differences, the process in Scheme 2 was dissected into its specific components. Figure 9 shows the emission from solutions of [$\mathbf{C_8}$] = 1.2×10^{-7} M when in the presence of ss-DNA_5-C* (5′-C*-ATC TTG ACT ATG TGG GTG CT-3′, C* = fluorescein) or hybridized-DNA_5-C* (ss-DNA_5-C*/ss-DNA_6, ss-DNA_6: 5′-AGC ACC CAC ATA GTC AAG AT-3′) under similar conditions. A higher FRET ratio is observed for ss-DNA_5-C* than for hybridized DNA_5-C*. These data are consistent with a stronger attraction between $\mathbf{C_8}$ and ss-DNA_5-C*. When [$\mathbf{C_8}$] increases, the FRET ratios for hybridized-DNA_5-C* and ss-DNA_5-C* become more equal. As shown by Figure 10, by the time that [$\mathbf{C_8}$] = 2.3×10^{-7} M and [ss-DNA_5-C*] = 2.0×10^{-8} M or [hybridized DNA_5-C*] = 2.0×10^{-8} M, the FRET ratios are nearly the same.

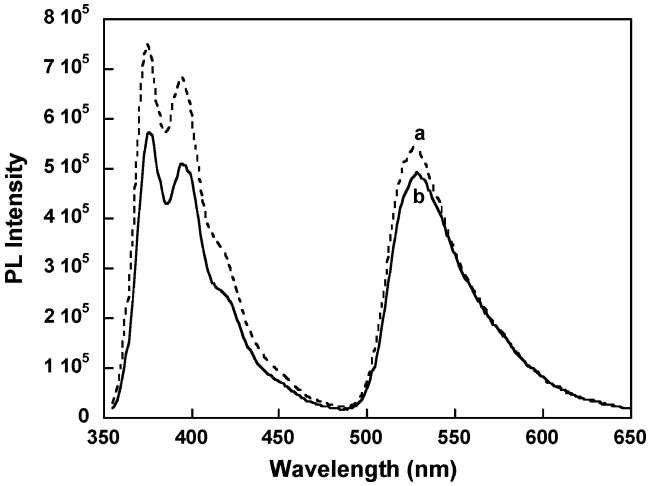

Figure 10. Emission spectra from solutions containing $\mathbf{C_8}$ and (a) ss-DNA_5-C* and (b) hybridized DNA_5-C* in buffer ([ss-DNA_5-C*] or [hybridized DNA_5-C*] = 2.0×10^{-8} M, [$\mathbf{C_8}$] = 2.3×10^{-7} M). The excitation wavelength used was 345 nm.

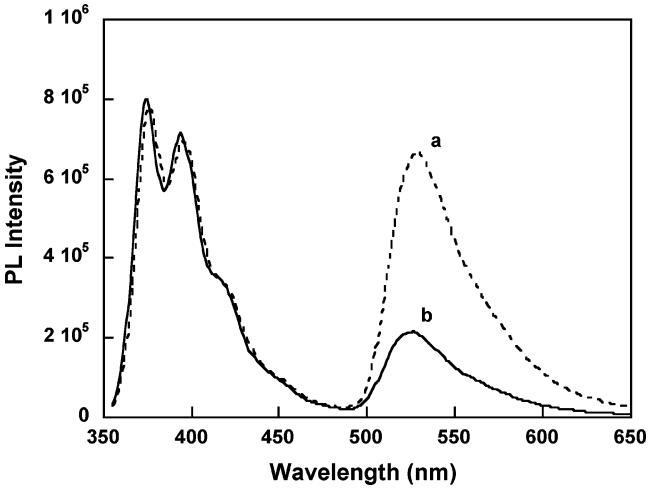

Figure 11. Emission spectra from solutions containing $\mathbf{C_8}$ and (a) hybridized DNA_5-C* and (b) ss-DNA_5-C* + ss-DNA_7 in buffer ([ss-DNA_5-C*] or [hybridized DNA_5-C*] = 2.0×10^{-8} M, [$\mathbf{C_8}$] = 2.3×10^{-7} M). The spectra are normalized with respect to the $\mathbf{C_8}$ emission.

Comparison of the C* emission from $\mathbf{C_8}$/hybridized DNA_5-C* against that from $\mathbf{C_8}$/ss-DNA_5-C* in the presence of noncomplementary ss-DNA_7 (5′-GAC TCA ATG GCG TTA GAC TG) shows more efficient energy transfer in the case of hybridized DNA_5-C* (Figure 11). The lower FRET observed when in the presence of the noncomplementary strand must arise from a competition between ss-DNA_5-C* and the unhybridized ss-DNA_7, rather than a stronger attraction between $\mathbf{C_8}$ and hybridized DNA_5-C*, relative to ss-DNA_5-C*. The success of Scheme 2 does not rely on a stronger interaction between the CCP and ds-DNA, relative to ss-DNA.

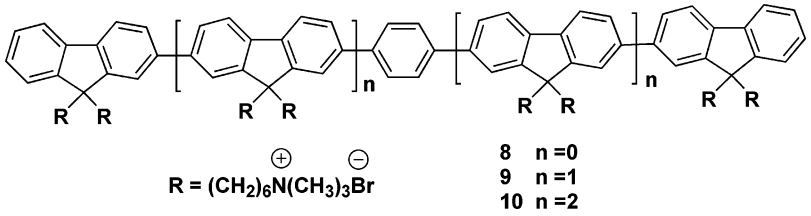

Figure 12. Chemical structures of oligomers **8**−**10**.

Scheme 3. Electrostatic Interactions between a CCP and RNA/Protein-C* Pairs (Graphic Used with Permission[46])

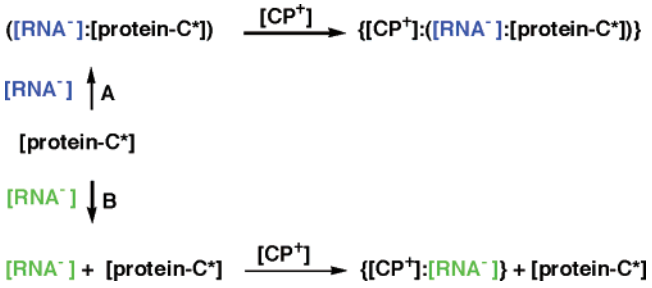

Scheme 4. Chemical Structures of Polymer 11, Tat-C*, SH3-C*, TAR RNA, and dTAR RNA (Graphic Used with Permission[46])

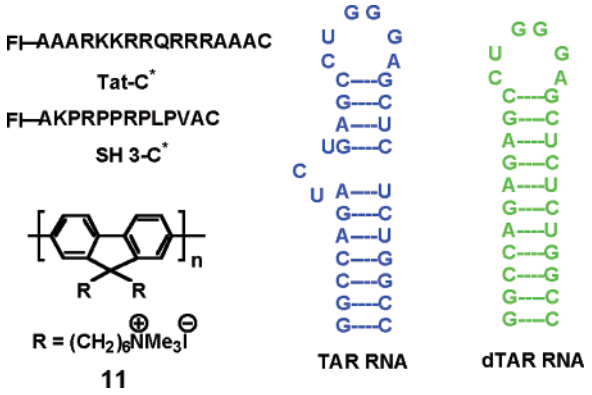

Rather, more efficient FRET occurs with hybridized DNA-C* because in situation **B** the nonhybridized strands that remain in solution screen the interaction between the CCP and ss-DNA-C*.

Molecules **8**−**10** (Figure 12) were designed to understand how the interactions of conjugated polymers with DNA structures vary with the number of monomer repeat units. The comparison is based on oligomer fluorescence quenching (ss-DNA_5 or hybridized DNA_5/DNA_6 titration) and energy-transfer experiments (ss-DNA_5-C* or hybridized-DNA_5-C* as the acceptor).[46] It was found that, normalized to the number of DNA charge units, ss-DNA_5 quenches the emission of **8**−**10** more efficiently than hybridized DNA, probably as a result of the increased hydrophobic interactions and its more flexible structure. For **8** and **9**, the quenching by fluorescein is more effective when bound to ss-DNA, relative to ds-DNA, while the opposite is true for **10**. The DNA/**8**−**10** interactions are therefore size-specific and sensitive to the DNA structure.

Fluorescence-Amplified Protein−RNA Detection

Similar to using PNA-C* or DNA-C* as a signaling probe, a homogeneous RNA detection method that

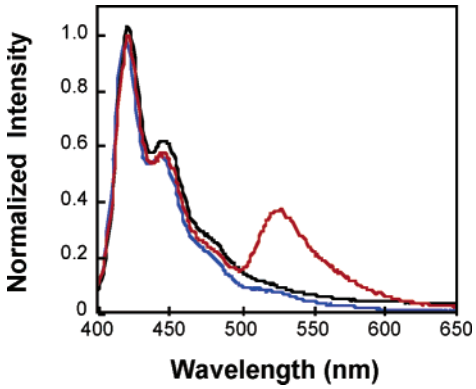

Figure 13. Emission spectra from solutions containing **11** and Tat-C*/TAR RNA (red), Tat-C*/dTAR RNA (blue), SH3-C*/TAR RNA (black), λ_{ex} = 380 nm, [**11**] = 9.6 × 10^{-7} M in RUs. Measurements are in tris-EDTA buffer solution (10 mM, pH = 7.4). The spectra are normalized with respect to the emission of **11**. Figure used with permission.[46]

couples the specificity of RNA/peptide binding events with the optical amplification of conjugated polymers has been designed.[47] The concept was illustrated using the binding of the transactivator (Tat) peptide to the transactivation responsive element RNA sequence (TAR RNA) of HIV-1.[48]

Scheme 3 reiterates the important role of electrostatic interactions.[30] One starts by mixing the protein-C* with the RNA in solution. Situation **A** corresponds to the RNA sequence (shown in blue) which specifically binds protein-C*. Upon binding, C* is attached to an RNA/protein macromolecule that differs in charge from protein-C* by the negative charge intrinsic to the RNA. For the detection scheme to work, the *net* charge in the RNA/protein complex must be negative. Situation **B** shows that, with a nonbinding RNA sequence (green), protein-C* remains separate, and there is no net change in charge in the vicinity of C*. In **A**, the CCP resides close to C*. In **B**, the RNA and the CCP come together, but remain separated from protein-C*.

The RNA and protein chosen for this study were the HIV-1 mRNA fragment, TAR RNA, and its specific Tat polypeptide. The specific molecular structures of RNAs and the labeled proteins and the cationic poly(fluorene) **11** are shown in Scheme 4.[49] The bulge structure in TAR RNA is a requirement for Tat binding.[50] A nonspecific polypeptide sequence labeled with fluorescein at the N-terminus (SH3-C*) and a three base mutation dTAR RNA were also chosen for comparison.

As shown in Figure 13, when **11** serves as the donor, C* emission is difficult to detect for the nonbinding pairs Tat-C*/dTAR RNA and SH3-C*/TAR RNA. For the Tat-C*/TAR RNA pair, the fluorescein emission using 380-nm excitation is 10 times larger than that obtained by excitation at the Tat-C* absorption maximum (480 nm) in the absence of the donor. The data demonstrate

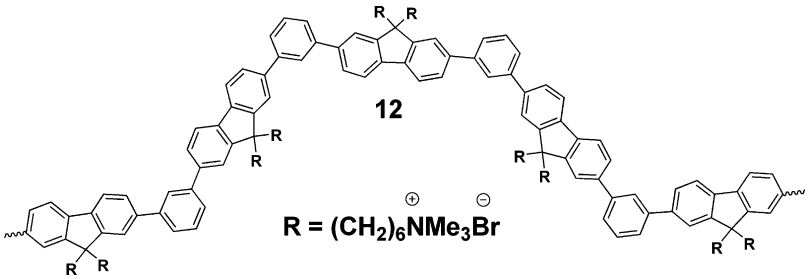

Figure 14. Example of cationic polymer with "kinked" structures.

amplified fluorescence and selective detection of TAR RNA.

Modified Conjugated Polymer Structures for Improved Detection Sensitivity and Selectivity

Based on the successful demonstration of using CCP-amplified fluorescence energy transfer, further modifications of the polymer structure were made to fine-tune spectral overlap and spatial proximity. Conjugated polymers frequently take the form of rigid-rod structures, which have limited flexibility and limited spatial registry with the three-dimensional molecular shapes of DNA, RNA and proteins. A backbone such as that of polymer **12** (in Figure 14), with a 120° orientation between fluorenyl units, would be expected to have more conformational freedom and improved registry with analyte shape.[51]

The introduction of nonlinear "kinks" along a linear polymer structure is accomplished by varying the ratio of *p*- and *m*-phenyl linkages at the synthesis stage. The corresponding polymers are abbreviated as $M_nP_m^+$, where the subscripts in M_n and P_m correspond to the percentage of *meta* units and *para* units in the backbone. There is a progressive blue shift in absorption with increasing meta content, while increasing the para content past the 50:50 ratio does not perturb the emission maxima. Fast energy transfer, either by intra- or interchain mechanisms, localizes excitations on the longest conjugation segments within the lifetime of the excited state.[52]

The FRET efficiency from $M_{50}P_{50}^+$ or $M_0P_{100}^+$ to hybridized DNA$_5$-C* was examined, as shown in Figure 15, where the C* emission intensity is plotted as a function of polymer concentration. Excitation at 363 nm leads to a similar number of polymer-based excited states. The data in Figure 15 show more efficient FRET from the $M_{50}P_{50}^+$, consistent with a shorter distance to hybridized DNA$_5$-C*, and/or with more variable orientations of the transition moments (improved ϵ in the FRET equation).

A second set of experiments involved FRET from the polymers to ds-DNA (ss-DNA$_5$/ss-DNA$_6$) with intercalated ethidium bromide (EB).[53,54] EB emission occurs only by FRET from the CCPs to the intercalated moieties. Figure 16 shows more efficient transfer in the series $M_0P_{100}^+ \rightarrow M_{25}P_{75}^+ \rightarrow M_{50}P_{50}^+ \rightarrow M_{75}P_{25}^+$ ($M_{100}P_0^+$ was not tested because its emission spectrum does not overlap significantly the absorption spectra of EB). A clear improvement in FRET therefore takes place with increased meta content in the polymer.

Efforts have also been made to tune the conjugated polymer emission to match different probe chromophores.[55] Recent experimental and theoretical studies indicate that energy transfer *between* segments in conjugated polymers may be substantially more important than along the backbone.[56,57] External perturbations that decrease backbone elongation, or that bring segments closer together, can be used to substantially modify the emissive properties of a polymer in solution. With these considerations in mind, polymer **13** (Figure 17) was prepared, which contains a small number of 2,1,3-benzothiadiazole (BT) chromophores within the original structure of polymer **5**.

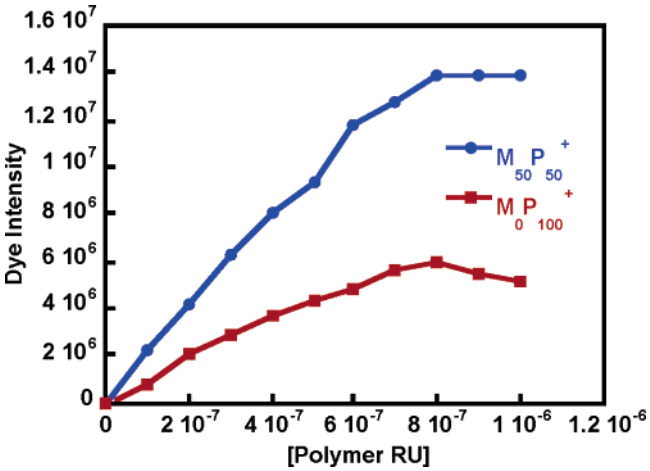

Figure 15. C* emission intensity vs polymer concentration for $M_{50}P_{50}^+$/hybridized-DNA$_5$-C* (blue) and $M_0P_{100}^+$/ hybridized-DNA$_5$-C* (red) in 50 mmol of phosphate buffer (pH = 8.0) at a [hybridized-DNA$_5$-C*] = 2.0×10^{-8} M.

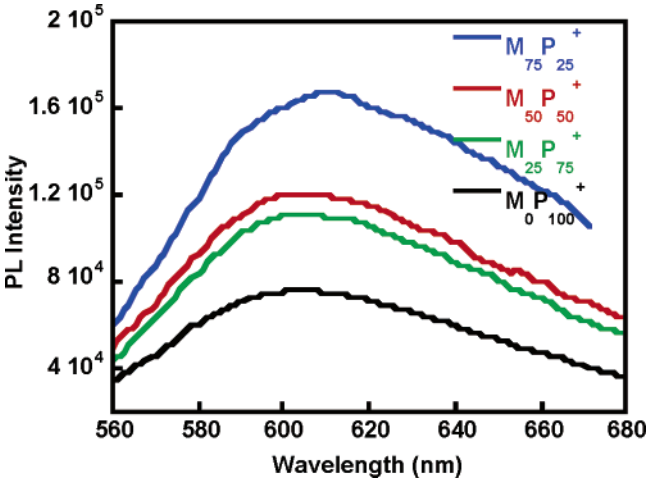

Figure 16. Comparison of the EB emission intensity for CCPs/ds-DNA/EB in 50 mmol of phosphate buffer (pH = 7.4) with [ds-DNA] = 1.0×10^{-8} M, [RU] = 2.0×10^{-7} M, [EB] = 1.1×10^{-6} M. Emission intensity was normalized relative to the ϵ value at the excitation wavelength.

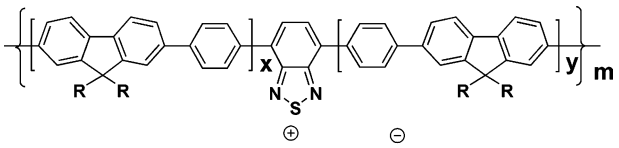

13

Figure 17. Chemical structure of polymer **13**.

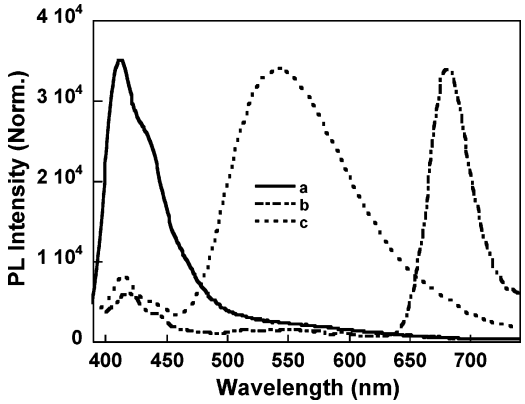

Figure 18. Normalized fluorescence in water of (a) **13/**PNA-Cy5, (b) **13/**ss-DNA_8 + PNA-Cy5, and (c) **13/**ss-DNA_9/PNA-Cy5 ([PNA-Cy5] = 2.0×10^{-8} M, [RU] = 1.6×10^{-7} M (λ_{exc} = 380 nm).

In dilute solution the emission of **13** is blue (λ_{max} = 410 nm). Upon addition of ss-DNA or ds-DNA, the emission shifts to a green color characteristic of the BT chromophore. Electrostatic complexation with negatively charged DNA results in polymer aggregation, a reduction of the average intersegment distance and an improved FRET to the green emitting sites.

With the aid of a PNA-C* (5′-C*-CAGTCCAGTGATACG, C* = Cy5, where Cy5 is a standard red emitting dye) probe strand, one can obtain three different colors, depending on the solution content: blue, in the absence of DNA; green, when noncomplementary ss-DNA_8 (5′-ACTGACGATAGACTG) is present; and red, when the complementary ss-DNA_9 (5′-CGTATCACTGGACTG) is found (Figure 18).

Summary

The recent reports summarized in this review show that electrostatic interactions between conjugated polyelectrolytes and negatively charged DNA or RNA can be used to modify optical properties and thereby detect hybridization states. In the case of cationic poly(thiophene) derivatives, one observes changes that arise from structural changes on the conjugated polymer structure. Complexation events that give rise to more planar backbone structures red-shift absorption and emission and modify emission efficiencies. In the case of poly(fluorene-*co*-phenylene) derivatives, electrostatic complexation determines intermolecular distances and controls FRET efficiencies. From a practical perspective, the polymer behaves as a light-harvesting structure that can be used to amplify the emission intensities of diagnostic chromophores and should allow interrogation of samples that are difficult to detect using standard single fluorophore assays. Use of conjugated polymers does not require sophisticated instrumentation and should be applicable to many standard fluorescent assays. Fine-tuning of these electrostatic and optical events should lead to multicolor biosensors for real-time applications. Clear challenges for widespread implementation include the synthesis of water-soluble conjugated polymers with a range of emission frequencies, large quantum efficiencies, and specific molecular structures that more clearly differentiate DNA's secondary and tertiary structures.

References

(1) Wang, J. *Nucleic Acid Res.* **2000,** *28*, 3011.
(2) Umek, R. M.; Lin, S. W.; Vielmetter, J.; Terbrueggen, R. H.; Irvine, B.; Yu, C. J.; Kayyem, J. F.; Yowanto, H.; Blackburn, G. F.; Farkas, D. H.; Chen, Y. P. *J. Mol. Diag.* **2001,** *3*, 74.
(3) Schork N. J.; Fallin D.; Lanchbury J. S. *Clini. Genet.* **2000,** *58*, 250.
(4) (a) Dubertret, B.; Calame, M.; Libchaber, A. *Nat. Biotechnol*. **2001**, *19*, 365. (b) Cardullo, R. A.; Agrawal, S.; Flores, C.; Zamecnik, P. C.; Wolf, D. E. *Proc. Natl. Acad. Sci. U.S.A.* **1988**, *85*, 8790.
(5) Balakin, K. V.; Korshun, V. A.; Mikhalev, I. I.; Maleev, G. V.; Malakhov A. D.; Prokhorenko, I. A.; Berlin, Yu. A. *Biosens. Bioelectron.* **1998,** *13*, 771.
(6) (a) Fodor, S. P.; Read, J. L.; Pirrung, M. C.; Stryer, L.; Lu, A. T.; Solas, D. *Science* **1991**, *251*, 767. (b) Livache, T.; Roget, A.; Dejean, E.; Barthet, C.; Bidan, G.; Teoule, R. *Nucleic Acids Res.* **1994**, *22*, 2915. (c) Tyagi, S.; Kramer, F. R. *Nat. Biotechnol*. **1996**, *14*, 303. (d) Millan, K. M.; Mikkelsen, S. R. *Anal. Chem.* **1993**, *65*, 2317. (e) Taton, T. A.; Mirkin, C. A.; Letsinger, R. L. *Science* **2000**, *289*, 1757.
(7) Niemeyer, C. M.; Blohm, D. *Angew. Chem., Int. Ed.* **1999**, *38*, 2865.
(8) Gerion, D.; Parak, W. J.; Williams, S. C.; Zanchet, D.; Micheel, C. M.; Alivisatos, A. P. *J. Am. Chem. Soc.* **2002**, *124*, 7070.
(9) Bruchez, M.; Moronne, M.; Gin, P.; Weiss, S.; Alivisatos, A. P. *Science* **1998**, *281*, 2013.
(10) Chan, W. C. W.; Nie S. M. *Science* **1998**, *281*, 2016.
(11) He, L.; Musick, M. D.; Nicewarner, S. R.; Salinas, F. G.; Benkovic, S. J.; Natan, M. J.; Keating, C. D. *J. Am. Chem. Soc.* **2000**, *122*, 9071.
(12) Nelson, B. P.; Grimsrud, T. E.; Liles, M. R.; Goodman, R. M.; Corn, R. M. *Anal. Chem*. **2001**, *73*, 1.
(13) Tombelli, S.; Minunni, M.; Mascini, M. *Anal. Lett.* **2002**, *35*, 599.
(14) (a) Patolsky, F.; Weizmann, Y.; Willner, I. *J. Am. Chem. Soc.* **2002**, *124*, 770. (b) Caruana, D. J.; Hellerr. A. *J. Am. Chem. Soc.* **1999**, *121*, 769.
(15) Lakowicz, J. R. *Principles of Fluorescence Spectroscopy*, 2nd ed.; Kluwer Academic/Plenum Publishers: New York, 1999.
(16) Sueda, S.; Yuan, J.; Matsumoto, K. *Bioconjugate Chem*. **2002**, *13*, 200 and references therein.
(17) Paris, P. L.; Langenhan, J. M.; Kool, E. T. *Nucleic Acids Res.* **1998**, *26*, 3789.
(18) LePecg, J. B.; Paoletti, C. *J. Mol. Biol.* **1967**, *27*, 87.
(19) Petty, J. T.; Bordelon, J. A.; Robertson, M. E. *J. Phys. Chem. B* **2000**, *104*, 7221.
(20) Cardullo, R. A.; Agrawal, S.; Flores, C.; Zamechnik, P. C.; Wolf, D. E. *Proc. Natl. Acad. Sci. U.S.A.* **1988**, *85*, 8790.
(21) Castro, A.; Williams, J. G. K. *Anal. Chem.* **1997**, *69*, 3915.
(22) (a) Guillet, J. E. *Polymer Photophysics and Photochemistry*; Cambridge University Press: Cambridge, 1985. (b) Kauffmann, H. F. *Photochemistry and Photophysics*; Radek, J. E., Ed.; CRC Press: Boca Raton, FL, 1990; Vol. 2. (c) Scholes, G. D.; Ghiggino, K. P. *J. Chem. Phys.* **1994**, *101*, 1251. (d) Weber, S. E. *Chem. Rev*. **1990**, *90*, 1469.
(23) Heeger, P. S.; Heeger, A. J. *Proc. Natl. Acad. Sci. U.S.A.* **1999**, *96*, 12219.
(24) (a) Leclerc, M. *Adv. Mater*. **1999**, *11*, 1491. (b) McQuade, D. T.; Pullen, A. E.; Swager, T. M. *Chem. Rev.* **2000**, *100*, 2357. (c) Chen, L.; McBranch, D. W.; Wang, H. L.; Hegelson, R.; Wudl, F.; Whitten, D. C. *Proc. Natl. Acad. Sci. U.S.A.* **1999**, *96*, 12287. (d) Ewbank, P. C.; Nuding, G.; Suenaga, H.; McCullough, R. D.; Shinkai, S. *Tetrahedron Lett.* **2001**, *42*, 155.
(25) (a) Korri-Youssoufi, H.; Garnier, F.; Srivastava, P.; Godillot, P.; Yassar, A. *J. Am. Chem. Soc.* **1997**, *119*, 7388. (b) Bäuerle, P.; Emge, A. *Adv. Mater*. **1998**, *10*, 324. (c) Garnier, F.; Korri-Y, H.; Srivastava, P.; Mandrand, B.; Delair, T. *Synth. Met*. **1999**, *100*, 89. (d) Korri-Y., H.; Yassar, A. *Biomacromolecules* **2001**, *2*, 58.
(26) Ho, H. A.; Boissinot, M.; Bergeron, M. G.; Corbeil, G.; Doré, K.; Boudreau, D.; Leclerc, M. *Angew. Chem., Int. Ed*. **2002**, *41*, 1548.
(27) Pinto, M. R.; Schanze, K. S. *Synthesis-Stuttgart*. **2002**, *9*, 1293.
(28) Traser, S.; Wittmeyer, P.; Rehahn, M. *e-Polymer* **2002**, *32*, 1.

(29) Kabanov, A. V.; Felgner, P.; Seymour, L. W. Eds. *Self-assembling Complexes for Gene Delivery. From Laborotary to Clinical Trial*; John Wiley: Chichester, 1998.
(30) Bronich, T. K.; Nguyen, H. K.; Eisenberg, A.; Kabanov, A. V. *J. Am. Chem. Soc.* **2000**, *122*, 8339.
(31) Although anionic poly(phenyleneethynylene), such as biotinylated PPEs (**1** in Figure 1), have also been used for DNA analysis, strepavidine-derivated polystyrene microspheres are required to bind both polymers and biotinylated probes. See references: (a) Kushon, S. A.; Ley, K. D.; Bradford, K.; Jones, R. M.; McBranch, D.; Whitten, D. *Langmuir* **2002**, *18*, 7245. (b) Kushon, S. A.; Bradford, K.; Marin, V.; Suhrada, C.; Armitage, B. A.; McBranch, D.; Whitten, D. *Langmuir* **2003**, *19*, 6456.
(32) Leclerc, M.; Ho, H. A.; Boissinot, M. WO 02/081735 A2, 2002.
(33) Peter, K.; Nilsson, R.; Inganäs, O. *Nat. Mater*. **2003**, *2*, 419.
(34) Doré, K.; Dubus, S.; Ho, H. A.; Lévesque, I.; Brunette, M.; Corbeil, G.; Boissinot, M.; Boivin, G.; Bergeron, M. G.; Boudreau, D.; Leclerc, M. *J. Am. Chem. Soc.* **2004**, *126*, 4240.
(35) Gaylord, B. S.; Heeger A. J.; Bazan G. C. *Proc. Natl. Acad. Sci. U.S.A.* **2002**, *99*, 10954.
(36) Förster, T. *Ann. Phys.* **1948**, *2*, 55.
(37) Stork, M. S.; Gaylord, B. S.; Heeger, A. J.; Bazan, G. C. *Adv. Mater.* **2002**, *14*, 361.
(38) Gaylord, B. S.; Heeger A. J.; Bazan G. C. *J. Am. Chem. Soc.* **2003**, *125*, 896.
(39) Israelachvili, J. *Intermolecular & Surface Forces*; Academic Press: London, 1992.
(40) This result indicates that the rigid polyfluorene structure most likely does not adapt to the DNA conformation upon complexation. They also suggest that binding into the grooves of DNA, like other cationic dyes such as ethidium bromide, is not a dominant form of association. Any twisting to accommodate such groove binding or helical conformation would likely shorten the effective conjugation length in the conducting polymer and thus blue-shift the emission. This information strengthens the idea that interactions between DNA and **4** are largely due to electrostatics.
(41) Liu, B.; Gaylord, B. S.; Wang, S.; Bazan, G. C. *J. Am. Chem. Soc.* **2003**, *125*, 6705.
(42) Wang, J.; Wang, D.; Miller, E. K.; Moses, D.; Bazan, G. C.; Heeger, A. J. *Macromolecules* **2000**, *33*, 5153.
(43) Matulis, D.; Rouzina, I.; Bloomfield, V. A. *J. Am. Chem. Soc*. **2002**, *124*, 7331.
(44) Pullman, B.; Lavery, R.; Pullman, A. *Eur. J. Biochem.* **1982**, *124,* 229.
(45) Diogo, M. M.; Queiroz, J. A.; Monteiro, G. A.; Martins, S. A. M.; Ferreira, G. N. M.; Prazeres, D. M. F. *Biotechnol. Bioeng*. **2000**, *68*, 576.
(46) Wang, S.; Liu, B.; Gaylord, B. S.; Bazan, G. C. *Adv. Funct. Mater*. **2003**, *13*, 463.
(47) Wang, S.; Bazan, G. C. *Adv. Mater*. **2003**, *15*, 1425.
(48) (a) Chen, L.; Frankel, A. D.; *Proc. Natl. Acad. Sci. U.S.A.* **1995**, *92*, 5077. (b) Leulliot, N.; Varani, G. *Biochemistry* **2001**, *40*, 7949.
(49) Richter, S.; Cao, H.; Rana, T. M. *Biochemistry* **2002**, *41*, 6391.
(50) Puglisi, J. D.; Tan, R.; Calnan, B. J.; Frankel, A. D.; Williamson, J. R. *Science* **1992**, *257*, 76.
(51) Liu, B.; Wang, S.; Bazan, G. C.; Mikhailovsky, A. *J. Am. Chem. Soc*. **2003**, *125*, 13306.
(52) Miao, Y. J.; Herkstroeter, W. G.; Sun, B. J.; Wong-Foy, A. G.; Bazan, G. C. *J. Am. Chem. Soc.* **1995**, *117*, 11407.
(53) LePecg, J. B.; Paoletti, C. *J. Mol. Biol.* **1967**, 27, 87.
(54) Morgan, A. R.; Pulleyblank, D. E. *Biochem. Biophys. Res. Commun.* **1974**, *61*, 346.
(55) Liu, B.; Bazan, G. C. *J. Am. Chem. Soc.* **2004**, *126*, 1942.
(56) Beljonne, D.; Pourtois, G.; Silva, C.; Hennebicq, E.; Herz, L. M.; Friend, R. H.; Scholes, G. D.; Setayesh, S.; Mullen, K.; Bredas, J. L. *Proc. Natl. Acad. Sci. U.S.A.* **2002**, *99*, 10982.
(57) Nguyen, T. Q.; Wu, J. J.; Doan, V.; Schwartz, B. J.; Tolbert, S. H. *Science* **2000**, *288*, 652.

CM049587X